ISSN: 1813-4890

# Research on the Optimized Design of Variable-Pitch Screw Rotor Profiles in Vacuum Pumps

Yuefei Zheng, Yushuang Feng*, Jiajun Su and Bo Yuan

School of Mechanical Engineering, Tianjin University of Technology and Education, Tianjin 300222, China

## Abstract

**To address challenges such as cusp points at tooth tips and oversized leakage channels in variable-pitch screw rotor designs, this study proposes an optimized rotor profile. The optimized end-face geometry consists of an addendum arc, dedendum arc, involute, extended epicycloid, and three transitional arcs. This design eliminates cusp points and reduces leakage paths, thereby improving volumetric efficiency. A mathematical model of the cylindrical helical curve for the variable-pitch rotor is established, with parametric equations derived to ensure continuity and smooth transitions between pitch segments. A 3D model of the optimized rotor is created, and comparative CFD simulations are performed. Simulation results indicate that the optimized rotor delivers significantly enhanced internal compression performance, with a 49.2% improvement over the conventional design. This study offers theoretical guidance for rotor profile optimization and contributes to enhanced performance and reliability of variable-pitch screw vacuum pumps.**

## Keywords

**Variable Pitch, Screw Vacuum Pump, Profile Optimization, Parametric Equation.**

## 1. Introduction

Variable-pitch screw vacuum pumps are a promising category of dry vacuum pumps [1]. Compared with conventional oil-sealed pumps—such as rotary vane and slide valve types—they offer a wide range of pumping speeds, compact design, oil-free operation, extended service life, low energy consumption, and broad applicability in the semiconductor, pharmaceutical, food, and chemical industries [2–4]. As the core pumping component, the rotor profile has a significant impact on pump performance, operational lifespan, and manufacturing costs, accounting for nearly half of the total production cost. Single-head variable-pitch screw rotors, characterized by internal pre-compression discharge, offer superior energy efficiency and noise reduction compared to equal-pitch counterparts. These advantages have attracted considerable attention from design engineers [5–7]. However, the immaturity of profile design theory, technical confidentiality, and the scarcity of publicly available information have hindered further development [8–10]. Recent studies have primarily focused on optimizing rotor profiles. Li Ming [11] proposed an innovative method for optimizing dry screw vacuum pump rotor profiles by refining geometric parameters. Wang Xiaodong [12] performed multi-objective optimization through simulations and experiments, leading to reduced leakage and improved compression performance. Zhang Ming [13] utilized multiphysics coupling analysis for profile optimization, which reduced energy consumption and enhanced operational stability. Smith [14] applied both computational and experimental methods to optimize rotor profiles, resulting in significant improvements in both pumping capacity and compression efficiency. Although rotor profile design is critical for improving efficiency and achieving high vacuum levels, comprehensive research on its adaptability and universality remains limited.

ISSN: 1813-4890

This paper analyzes and optimizes the end-face profile of a variable-pitch rotor, proposes an improved geometry, and derives its corresponding volumetric efficiency. The optimized helical curve is subsequently modeled to ensure geometric smoothness and continuity between pitch segments. Finally, computational fluid dynamics (CFD) simulations validate the enhanced performance of the optimized rotor, offering robust theoretical support for the advancement of variable-pitch screw vacuum pumps.

## 2. Analysis and Optimization of the Variable-Pitch Rotor End-Face Profile

### 2.1. Optimized Parametric Equations of the Variable-Pitch Rotor End-Face Profile

The end-face profile of the variable-pitch screw rotor consists of four segments: the addendum arc, the dedendum arc, and two transitional curves that connect these arcs. To ensure proper self-meshing, the transitional curves are designed based on gear engagement principles and typically include an involute and an extended epicycloid. Additional transitional arcs are incorporated between the addendum circle and the extended epicycloid, the addendum circle and the involute, and the dedendum circle and the involute. These arcs enhance meshing stability, reduce leakage, improve pumping efficiency, and decrease both noise and energy consumption. The structural diagram of the optimized end-face profile of the variable-pitch screw rotor is presented in Figure 1.

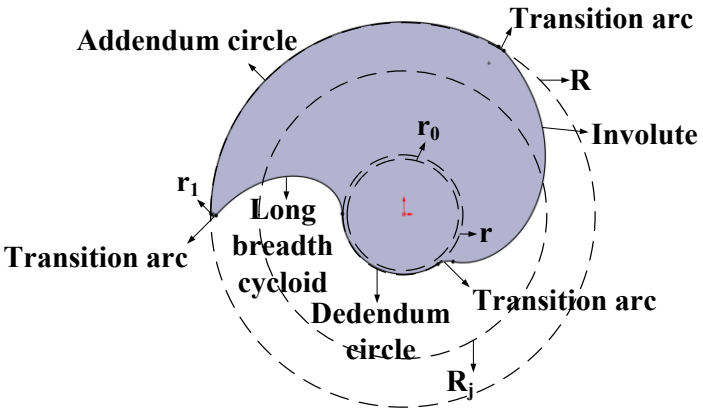


Figure 1: Structural Diagram of the Optimized End-Face Profile of the Variable-Pitch Screw Rotor

The parametric equations are as follows:

$$\begin{cases} x = 2 \times R_j \times \cos(t) + (R - r_1) \times \cos(2t) \\ y = 2 \times R_j \times \sin(t) - (R - r_1) \times \sin(2t) \end{cases} \tag{1}$$

Extended epicycloid:

$$\begin{cases} x = r \times \cos(t) \\ y = r \times \sin(t) \end{cases} \tag{2}$$

Dedendum arc:

$$\begin{cases} x = r_0 \times \cos(t) - r_0 \times t \times \sin(t) \\ y = r_0 \times \sin(t) + r_0 \times t \times \cos(t) \end{cases} \tag{3}$$

Involute:

$$\begin{cases} x = R \times \cos(t) \\ y = R \times \sin(t) \end{cases} \tag{4}$$

Addendum arc:

ISSN: 1813-4890

$$\begin{cases} x = r_1 \times \cos(t) \\ y = r_1 \times \sin(t) \end{cases} \tag{5}$$

Here, $t$ denotes the angular parameter; $R$ is the radius of the addendum circle; $R_j$ is the radius of the pitch circle; $r$ is the radius of the dedendum circle; $r_0$ is the base circle radius of the involute; and $r_1$ is the transitional arc radius. Figure 2 illustrates the meshing process of the optimized end-face geometry of the variable-pitch screw rotor. Compared with conventional end-face profiles, the optimized design eliminates cusp points at tooth tips and ensures smooth geometric transitions.

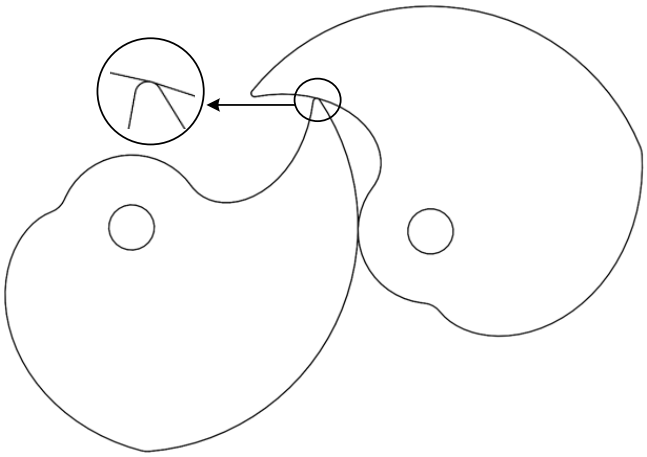

Figure 2: Meshing Process of the Optimized End-Face Profile of the Variable-Pitch Screw Rotor

Figure 3 shows the leakage channels formed during the meshing process. The size of these channels is significantly reduced, which enhances the ultimate vacuum level achievable by the variable-pitch screw vacuum pump.

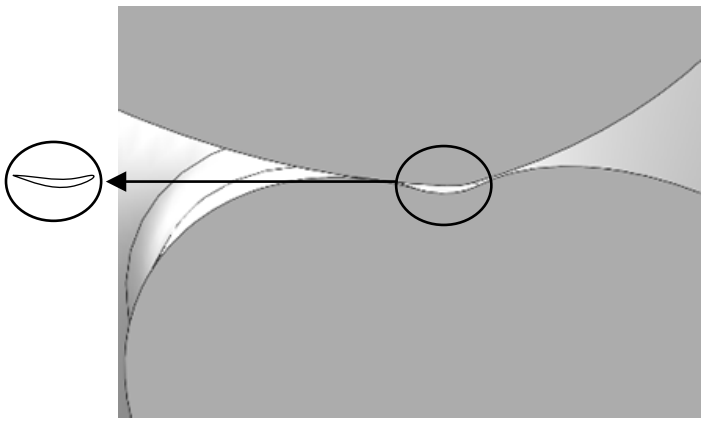

Figure 3: Leakage Channels Generated During the Meshing Process

## 2.2. Volumetric Efficiency of the Optimized Variable-Pitch Rotor End-Face

In the design of variable-pitch screw vacuum pumps, the volumetric efficiency of the end-face profile is a critical parameter for evaluating rotor performance. This metric reflects the ratio of the effective pumping area to the total cross-sectional area of the end face. A higher ratio indicates improved pumping efficiency and reduced energy consumption. To enhance volumetric efficiency, profile optimization must account for tooth geometry, rotor dimensions, and interlobe volume compatibility. A well-designed profile facilitates efficient gas transport, minimizes leakage, and ensures stable operation across a wide pressure range.

As shown in Figure 4, the schematic of the end-face cross-sectional area of the optimized variable-pitch screw rotor highlights the geometric characteristics of the improved profile and its influence on volumetric efficiency.

ISSN: 1813-4890

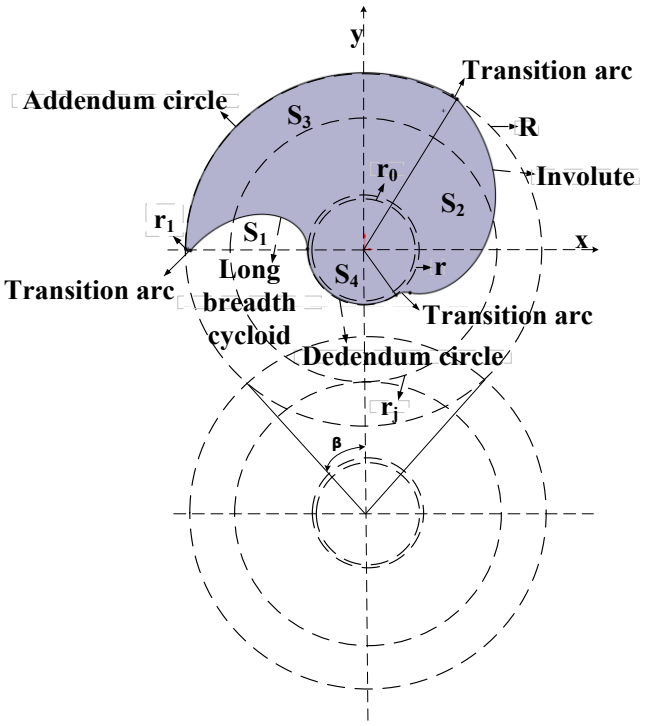


Figure 4: Schematic Diagram of the End-Face Area of the Optimized Variable-Pitch Screw Rotor

During operation, the male and female rotors engage to form a series of sealed chambers. The effective pumping area is defined as the cross-sectional area of the pump chamber excluding the areas occupied by the male and female rotor profiles. This effective area directly influences the overall pumping performance of the vacuum pump.

The cross-sectional area of the screw rotor is composed of five regions: $S_Z$, $S_1$, $S_2$, $S_3$, and $S_4$. These regions represent key geometric features, including the addendum, dedendum, and transitional curves. Due to the complexity of the profile curves, each region must be evaluated using integral analysis to obtain an explicit expression for the total cross-sectional area.

Accurate calculation of this area is critical for profile optimization and enhancing volumetric efficiency. The mathematical expressions corresponding to each segment of the rotor end-face profile are presented as follows:

$$S_1 = (2R_j^2 + R^2)\arccos(\frac{R_j}{R}) - 3R_j R\sin(\arccos(\frac{R_j}{R})) + R_j^2\sin(2\arccos(\frac{R_j}{R})) - R_j R\sin(3\arccos(\frac{R_j}{R})) + \frac{1}{4}R^2\sin(4\arccos(\frac{R_j}{R})) \quad (6)$$

$$S_2 = \frac{1}{6}r_0^2(\tan^3(\arccos(\frac{r_0}{R})) - \tan^3(\arccos(\frac{r_0}{r}))) \quad (7)$$

$$S_3 = \alpha_3 R^2 / 2 \quad (8)$$

$$S_4 = \alpha_4 r^2 / 2 \quad (9)$$

$$S_\infty = 2\pi R^2 - 2\beta R^2 + 4R_j^2\tan\beta \quad (10)$$

$$\beta = \arccos(\frac{R_j}{R}) \quad (11)$$

$S_1$: Area enclosed between the extended epicycloid and the rotor axis.

$S_2$: Area defined by the angular span of the involute segment.

$S_3$: Sector area defined by the addendum arc.

$S_4$: Sector area defined by the dedendum arc.

$\beta$: Meshing angle between the male and female rotors.

ISSN: 1813-4890

The volumetric efficiency *C* of the end-face profile is then expressed as:

$$C = 1 - 2(S_2 + S_3 + S_4 - S_1) / S_\infty \tag{12}$$

The volumetric efficiency *C* directly affects the pumping capacity of the vacuum pump. A higher volumetric efficiency enables a rotor of identical size to achieve greater theoretical pumping speeds, thereby improving the overall performance of the vacuum pump. Therefore, optimizing the profile of the variable-pitch screw rotor to increase volumetric efficiency is a critical strategy for enhancing vacuum pump performance.

## 3. Design of the Optimized Helical Unfolding Line of the Variable-Pitch Rotor

When the end-face profile remains constant during unfolding, the spatial geometry of the rotor is fully determined by the axial guide curve—specifically, the cylindrical helical line. Therefore, establishing a mathematical model of the cylindrical helical line is essential for rotor profile optimization. The cylindrical helical line in a variable-pitch screw rotor is a spatial curve whose pitch varies along the axial direction. This variable-pitch design enhances gas transport, improves internal compression efficiency, reduces energy consumption, and minimizes operational noise.

To accurately characterize the geometry of the optimized variable-pitch screw rotor, parametric equations are used to define the trajectory of the cylindrical helical line, thereby offering theoretical support for both profile optimization and manufacturing. The corresponding parametric equations are expressed as follows:

$$\begin{cases} x_i(t) = R\cos(t) \\ y_i(t) = R\sin(t) \qquad i = 1,2,3 \\ z_i(t) = f_i(t) \end{cases} \tag{13}$$

In the equation, t denotes the angular parameter representing the helical unfolding angle; R is the radius of the cylindrical helical line, which governs the curvature; and $f_i(t)$ is the parametric function along the z-axis for each segment, determining the pitch distribution. The unfolded schematic of the cylindrical helical line for the optimized variable-pitch screw rotor is presented in Figure 5.

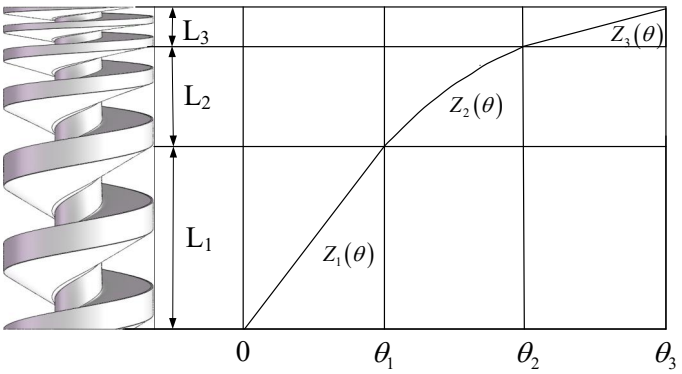


Figure 5: Unfolded Schematic of the Cylindrical Helical Line of the Optimized Variable-Pitch Screw Rotor

The continuity and smoothness of the cylindrical helical line are critical to ensuring pump stability and machining precision. To prevent abrupt changes or geometric discontinuities that degrade performance, the helical line must satisfy smooth transition conditions to optimize meshing characteristics and enhance pumping efficiency. Therefore, the helical line equation must fulfill the following parametric conditions to ensure smooth continuity and high-quality curve formation:

ISSN: 1813-4890

$$\begin{cases} f_1(\theta_1) = f_2(\theta_1) \\ f_1'(\theta_1) = f_2'(\theta_1) \\ f_1''(\theta_1) = f_2''(\theta_1) \\ f_2(\theta_2) = f_3(\theta_2) \\ f_2'(\theta_2) = f_3'(\theta_2) \\ f_2''(\theta_2) = f_3''(\theta_2) \end{cases} \tag{14}$$

Variations in pitch segments significantly influence the rotor's compression ratio and operational behavior. A mathematical model must be developed to describe the geometric relationships within each pitch segment, and corresponding parametric equations should be derived accordingly.

As illustrated in Figure 5, the optimized variable-pitch screw rotor is composed of multiple pitch segments, where $L_1$ and $L_3$ represent equal-pitch regions, and $L_2$ denotes the transitional segment. Let the lead of segment $L_1$ be $T_{max}$ and that of segment $L_3$ be $T_{min}$. Based on the mathematical properties of the helical line, the z-axis parametric equation for the cylindrical helical line in the equal-pitch region $L_1$ is given as follows:

$$z_1(\theta) = f_1(\theta) = \frac{T_{\max}}{2\pi}\theta \qquad 0 \le \theta \le \theta_1 \tag{15}$$

The z-axis parametric equation for the cylindrical helical line in the equal-pitch region $L_3$ is expressed as follows:

$$z_3(\theta) = f_3(\theta) = \frac{T_{\min}}{2\pi}(\theta - \theta_2) + f_2(\theta_2) \qquad \theta_2 \le \theta \le \theta_3 \tag{16}$$

Let ε denote the total internal compression ratio of the optimized variable-pitch screw rotor. Given that the end-face profile remains unchanged along the axial direction, and based on rotor meshing and gas compression principles, the following constraint equation is derived:

$$\varepsilon_t = \frac{T_{\max}}{T_{\min}} \tag{17}$$

Neglecting the internal distribution of the compression ratio and based on polynomial interpolation theory, a unique polynomial interpolation function that exactly passes through multiple discrete points can be constructed:

$$f_2(\theta) = a_1\theta^4 + a_2\theta^3 + a_3\theta^2 + a_4\theta + a_5 \tag{18}$$

To ensure the continuity and smoothness of the helical line, a derivative analysis of its parametric representation is required. Based on the parametric continuity conditions defined in Equation (14), the first- and second-order derivatives of $f_1(\theta)$, $f_2(\theta)$, and $f_3(\theta)$ are computed to characterize the velocity and acceleration properties of the curve. In the variable-pitch segment, geometric smoothness must be preserved, which requires that both the first- and second-order derivatives remain continuous at the segment boundaries. By combining the derivative expressions, a one-dimensional linear system is formulated to solve for the polynomial coefficients $a_1$, $a_2$, $a_3$, $a_4$, and $a_5$.

$$\begin{bmatrix} \theta_1^4 & \theta_1^3 & \theta_1^2 & \theta_1 & 1 \\ 4\theta_1^3 & 3\theta_1^2 & 2\theta_1 & 1 & 0 \\ 12\theta_1^2 & 6\theta_1 & 2 & 0 & 0 \\ 4\theta_2^3 & 3\theta_2^2 & 2\theta_1 & 1 & 0 \\ 12\theta_2^2 & 6\theta_2 & 2 & 0 & 0 \end{bmatrix} \begin{bmatrix} a_1 \\ a_2 \\ a_3 \\ a_4 \\ a_5 \end{bmatrix} = \begin{bmatrix} \frac{T_{\max}}{2\pi}\theta_1 \\ \frac{T_{\max}}{2\pi} \\ 0 \\ \frac{T_{\max}}{2\pi\varepsilon_t} \\ 0 \end{bmatrix} \tag{19}$$

ISSN: 1813-4890

This system of equations defines the mathematical parameters of the optimized variable-pitch helical line, ensuring compliance with predefined geometric constraints and preserving the rationality of the variable-pitch screw rotor model. The polynomial system given in Equation (19) is implemented in MATLAB, where the associated variables and coefficients are symbolically defined. Using the solve function, symbolic expressions for the polynomial coefficients are obtained.

$$\begin{cases} a_1 = \dfrac{T_{\max}(1-\varepsilon_t)}{4\varepsilon_t\pi(\theta_1-\theta_2)^3} \\ a_2 = \dfrac{T_{\max}(\theta_1+\theta_2)(\varepsilon_t-1)}{2\varepsilon_t\pi(\theta_1-\theta_2)^3} \\ a_3 = \dfrac{3T_{\max}\theta_1\theta_2(1-\varepsilon_t)}{2\varepsilon_t\pi(\theta_1-\theta_2)^3} \\ a_4 = \dfrac{T_{\max}(\theta_1^3-3\theta_1^2\theta_2+3\varepsilon_t\theta_1\theta_2^2-\varepsilon_t\theta_2^3)}{2\varepsilon_t\pi(\theta_1-\theta_2)^3} \\ a_5 = \dfrac{T_{\max}\theta_1^3(1-\varepsilon_t)(2\theta_2-\theta_1)}{4\varepsilon_t\pi(\theta_1-\theta_2)^3} \end{cases} \tag{20}$$

By substituting Equation (20) into Equations (18) and (16), the complete parametric representation of the cylindrical helical line is obtained. Given the parameters of the optimized end-face profile and helical design—such as the lead $T_{max}$ for segment $L_1$, the total internal compression ratio $\varepsilon_t$, and the helical unfolding angles $\theta_1$, $\theta_2$, and $\theta_3$ for the three segments—these values can be substituted into the equations to construct the complete three-dimensional model of the optimized variable-pitch screw rotor.

## 4. Numerical Analysis of the Optimized Variable-Pitch Screw Rotor

### 4.1. Three-Dimensional Modeling of the Optimized Variable-Pitch Screw Rotor

Utilizing the previously derived parametric equations and the specified parameters of the optimized end-face profile and helical design, a complete three-dimensional model of the optimized variable-pitch screw rotor is constructed, as illustrated in Figure 6.

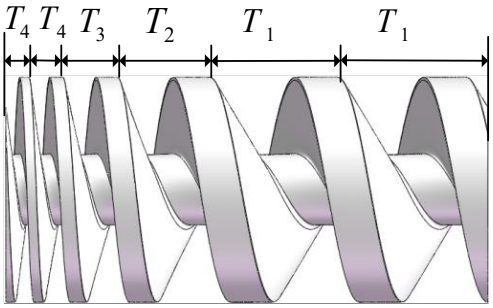


Figure 6: 3D Model of the Optimized Variable-Pitch Screw Rotor

The end-face profile remains invariant along the axial direction. The suction and discharge ends are composed of two equal-pitch segments, denoted as $T_1$ and $T_4$, respectively. The central region of the helical rotor contains a variable-pitch transitional segment, represented by $T_2$ and $T_3$. Smooth transitions are ensured at the interfaces between the three lead segments.

### 4.2. Fluid Dynamics Simulation of the Optimized Variable-Pitch Screw Rotor

The Flow Simulation module in SOLIDWORKS is employed to perform computational fluid dynamics (CFD) analysis on the optimized variable-pitch screw rotor. Initial conditions, including the rotor's rotational domain and boundary conditions, are defined to establish the simulation environment. The corresponding rotor simulation model is subsequently generated.

ISSN: 1813-4890

To ensure a valid performance comparison, a conventional variable-pitch screw rotor is simulated under identical parameters and boundary conditions. The same mesh resolution and pitch values are applied to both models to maintain consistency. Table 1 summarizes and compares the design parameters of the optimized and conventional variable-pitch screw rotors.

Table 1: Design Parameter Comparison Between Optimized and Conventional Variable-Pitch Screw Rotors

| Parameter | Optimized Rotor | Conventional Rotor |
|---|---|---|
| Iteration Count | 12996 | 7852 |
| Total Fluid Mesh Count | 68398 | 41467 |
| Fluid Mesh in Contact with Solid | 34926 | 24290 |
| X Dimension | 0.154 m | 0.154 m |
| Y Dimension | 0.076 m | 0.085 m |
| Z Dimension | 0.058 m | 0.078 m |
| High Mach Number Flow | No | No |
| Transient Analysis | Yes | Yes |

## 4.3. Comparative Analysis of Simulation Results

Both rotor models are subjected to transient internal flow field simulations over a duration of 5 seconds. The gas velocity streamlines within the optimized rotor are illustrated in Figure 7.

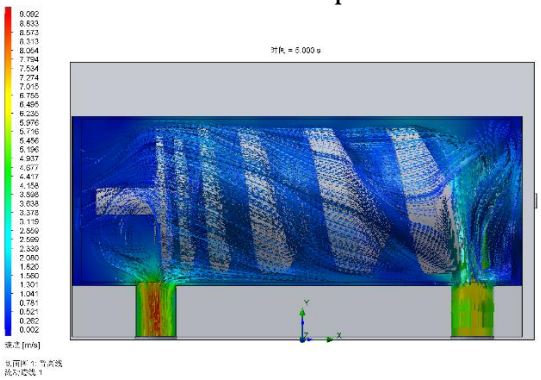

Figure 7: Gas Velocity Streamlines Inside the Optimized Variable-Pitch Screw Rotor

As shown in the velocity streamline diagram, the gas undergoes internal compression within the chamber of the optimized variable-pitch screw rotor, with the flow velocity increasing from 4.5 m/s at the inlet to 9.1 m/s at the outlet. The velocity streamline diagram for the conventional variable-pitch screw rotor is presented in Figure 8.

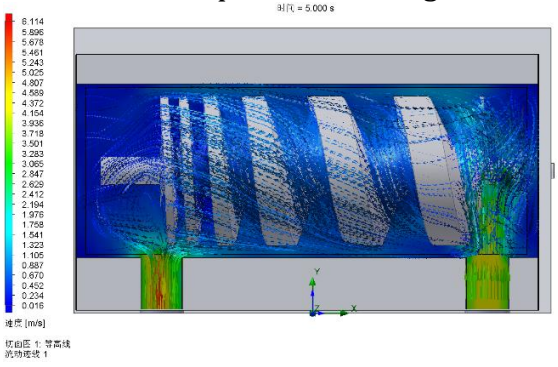

Figure 8: Gas Velocity Streamlines Inside the Conventional Variable-Pitch Screw Rotor

As shown in the velocity streamline diagram, the gas inside the chamber of the conventional variable-pitch screw rotor undergoes internal compression, with the flow velocity increasing from 4.5 m/s at the inlet to 6.1 m/s at the outlet. A comparison of inlet and outlet gas velocities for the optimized and conventional variable-pitch screw rotors is provided in Table 2.

ISSN: 1813-4890

Table 2: Presents the comparison of inlet and outlet gas velocities between the two models

| Parameter | Optimized Rotor | Conventional Rotor |
|---|---|---|
| Inlet Velocity (m/s) | 4.5 | 4.5 |
| Outlet Velocity (m/s) | 9.1 | 6.1 |

The comparison results indicate that, under identical parameter conditions, the optimized variable-pitch screw rotor exhibits significantly enhanced internal compression characteristics. Its performance improves by approximately 49.2% compared to the conventional design, thereby more effectively fulfilling the operational requirements of variable-pitch screw rotor applications.

## 5. Conclusion

This paper presents a comprehensive investigation into the optimized rotor profile design for a variable-pitch screw vacuum pump, and the key findings are summarized as follows:

(1) An optimized end-face profile for the variable-pitch rotor is proposed, which effectively eliminates cusp points at the tooth tips and ensures smooth geometric transitions. The improved profile reduces leakage during meshing, thereby significantly enhancing the ultimate vacuum level and providing a robust foundation for the overall performance improvement of the vacuum pump.

(2) A complete mathematical model of the cylindrical helical line is established to support the spiral unfolding design of the rotor. Parametric equations of the helical curve are derived for different pitch segments. Polynomial interpolation is employed to define the geometric relationships and variation patterns of the multi-segment pitch structure, ensuring continuity and smoothness of the helical line. This provides theoretical support for precise machining and improved operational stability of the optimized rotor.

(3) Numerical analysis and computational fluid dynamics (CFD) simulations are conducted to validate the effectiveness of the proposed optimization. Simulation results indicate that the optimized variable-pitch screw rotor exhibits significantly enhanced gas compression performance. The gas outlet velocity increases markedly, with overall performance improved by approximately 49.2% compared to the conventional design. This confirms the clear advantage of the optimized design in enhancing pump efficiency and reducing energy consumption. The findings provide robust theoretical support for further advancements in the design of variable-pitch screw rotor profiles.

## References

[1] R. Mehta and A. Khan: Experimental analysis of thermomechanical coupling in twin-screw vacuum pump rotors, Journal of Thermal Science and Engineering Applications, Vol. 15 (2022) No.1, p.011024.

[2] Y. Zhang and C. Li: Numerical simulation of thermal management in dry screw vacuum pumps, Journal of Thermal Science, Vol. 32 (2022) No.5, p.321-330.

[3] T. Liu and X. Wang: Performance optimization and thermodynamic analysis of twin-screw vacuum pumps, Journal of Vacuum Science & Technology A, Vol. 42 (2024) No.2, p.021301.

[4] R. Garcia and L. Martinez: Computational and experimental study on profile optimization for screw vacuum pumps, Journal of Vacuum Science & Technology A, Vol. 42 (2024) No.4, p.041301.

[5] X. Li and Y. Zhang: Investigation on thermal-structural coupling performance of CFRP rotors in screw vacuum pumps, International Journal of Heat and Technology, Vol. 40 (2022) No.2, p.215-230.

[6] S. Yang and J. Kim: Thermo-mechanical coupling analysis and optimization of screw vacuum pump rotors, ASME Journal of Engineering for Gas Turbines and Power, Vol. 146 (2024) No.6, p.061001.

[7] G. Chen and W. Zhang: Optimization of rotor profiles for improved performance in dry screw vacuum pumps, Vacuum, Vol. 185 (2024), p.107654.

[8] Z. Wang and J. Lee: Conductance and leak flow analysis in dry screw vacuum pumps using CFD, Journal of Process Mechanical Engineering, Vol. 236 (2022) No.3, p.347-360.

[9] D. Williams, T. Jackson and L. Garcia: Assessment of screw vacuum pump performance in pharmaceutical applications, Pharmaceutical Technology, Vol. 46 (2022) No.8, p.34-40.

[10] S. Huang, L. Fang and D. Chen: Design and simulation of screw vacuum pump for medical applications, Biomedical Engineering International, Vol. 56 (2023) No.3, p.421-430.

[11] M. Li, Q. Zhang and Y. Liu: High-efficiency dry screw vacuum pump rotor profile optimization design, Journal of Mechanical Engineering, Vol. 60 (2024) No.10, p.123-132.

[12] X. Wang, T. Liu and H. Li: Multi-objective optimization design of variable-pitch screw rotor profiles, Journal of Engineering Thermophysics, Vol. 45 (2024) No.8, p.987-996.

[13] M. Zhang, H. Li and X. Wang: Optimization design of screw rotor profiles based on multi-physics coupling, Journal of Vacuum Science and Technology, Vol. 44 (2025) No.3, p.456-465.

[14] A. Smith and J. Brown: Advanced profile optimization for screw vacuum pumps: a computational and experimental study, Journal of Vacuum Science & Technology A, Vol. 43 (2025) No.5, p.053401.